Influential Tokamak Datasets from L-mode International Database

B. Hu and W. Horton

Institute for Fusion Studies, The University of Texas at Austin, Austin, TX 78712

August 11, 2000

Abstract

The empirical tokamak energy confinement time τ_{E} is expressed in terms of the tokamak parameters in the form of power law scaling formulas. The international database, collected through the ITER project, yields the standard measure called the ITERL97-P confinement law [1] for baseline tokamak performance. We rederive the L-mode scaling formula from ITERL database and perform a statistical analysis for the prediction to larger tokamaks. A series of confinement times is generated by repeatedly performing the linear regression fit on the dataset dropping one machine each time. In this way, we can observe the influence of each particular machine on the empirical formula and the extrapolations made for the proposed IGNITOR and ITER-FEAT tokamak machines. The resulting spread in the predicted values of τ_{E} are 35% and 40% respectively for the two proposed machines IGNITOR and ITER-FEAT, and the influential machines defined as those which produce the largest changes when dropped from the database are discussed.

Future tokamaks for burning plasma experiments are compact and of high-density. In order to better predict their performance, a subset of the ITERL database, defined as the FUSP subdatabase, is used for linear regression and projection of the Lawson product for IGNITOR and ITER-FEAT design parameters.

F1 confinement and transport, global scaling

I. Introduction

The tokamak is a well documented engineering plasma confinement system that has been reproduced in laboratories through out the world for approximately thirty years. An important legacy of the ten-year ITER-EDA (engineering design analysis) project is the compilation and standardization of large international tokamak databases summarizing the performance as a function of size, shape and plasma control parameters. These historical databases give the best insight to the results of the large research and engineering investment made in the effort to produce controlled thermonuclear fusion.

The eight standard sets of machine and plasma variables used to describe the state of the low confinement mode plasma are defined in Table I. We use the parameter vector $\mu = \{M_{\rm eff}, R, a, \kappa, I_{\rm p}, B_{\rm T}, \langle n \rangle, P_{\rm L}\}$ to refer to the eight variables.

$$\tau_{\rm E} = e^{\rm const}\ M_{\rm eff}^{\alpha_M}\ R^{\alpha_R}\ a^{\alpha_a}\ \kappa^{\alpha_\kappa}\ B_{\rm T}^{\alpha_B}\ I_{\rm p}^{\alpha_I}\ n^{\alpha_n}\ P_{\rm L}^{\alpha_P}. \tag{1}$$

The power law form (1) for the empirical energy confinement time is widely used in the analysis of data and tokamak performance [1, 2, 3].

The parameters of IGNITOR [4], ITER-FEAT [5] and ITER-EDA [6] are listed in Table II. The objectives of this work are to use the baseline tokamak performance contained in the low (L-mode) confinement database to determine the uncertainties in the predicted confinement times for future machines. Here we concentrate on the predictions for three possible future tokamaks that are well advanced in their engineering design. The design parameters and the machine designer's estimate of the energy confinement are given in Table II for IGNITOR [4], ITER-FEAT [5, 7] and ITER [6]. The advanced operation scenarios planned for these machines require other parameters such as divertor parameters, magnetic and flow shear parameters which require consideration of additional parameters and shear profiles. Typically, advanced mode operational scenarios obtain a factor of two enhancement over the L-mode confinement time. The length of time for which the enhancement can be

sustained is poorly known. In a future work, we will extend the present analysis to the H-mode database where such issues are important. Here we restrict our consideration to the baseline tokamak operation.

In Section 2, we describe briefly the L-mode database, define the influential datasets, and give two estimates for the error in the standard ITERL97-P empirical confinement formula. In Section 3, we define the fusion power (FUSP) database that applies a filter to collect a dataset relevant to thermonuclear fusion. In Section 4, we discuss the results of the statistical analysis, compare the new empirical formula for the FUSP data with the standard ITERL97-P formula. We show that the probability distribution function for the confinement time data normalized to the FUSP empirical formula.

II. Influential Datasets and Estimation of Errors in the Scaling Law

The method of least squares is used as the maximum likehood estimator, after taking the logarithm of Eq. (1) for $\tau_{\rm E}$. First we use the entire database and reproduce Kaye's ITERL97-P formula. We use the whole dataset downloaded from Kaye in Feburary 2000. The dataset contains 1312 shots from 12 machines for the non-ohmic L-phase data with no Helium. The remaining shots are pure ohmic discharges for which the L-mode parameterization may not apply. The 12 tokamaks in the database are ASDEX, CMOD, D3D, JET, JFT2M, JT60U, PBXM, PDX, T10, TFTR, TXTR, TSUPRA. We obtain: $\alpha_M = 0.20$, $\alpha_R = 1.89$, $\alpha_a = -0.06$, $\alpha_\kappa = 0.64$, $\alpha_B = 0.03$, $\alpha_I = 0.96$, $\alpha_{\langle n \rangle} = 0.40$, $\alpha_P = -0.73$, in agreement with the values in Kaye *et al.* [1]. With the design parameters listed in Table II, we thus obtain the predicted confinement times for IGNITOR, ITER-FEAT and ITER using the ITERL97-P scaling.

Next we drop the data from a particular machine, and perform the same linear regression fit on the rest set of the data. The new scaling is then used to predict the confinement times.

The first column titled 97P in Table III gives the reference exponents and confinement times for all 1312 L-mode discharges. The titles of the rest of the columns in Table III are the names for the dropped machine. In this way, we can observe the influence of the data set of a particular machine on the empirical formula and extrapolations made for the three future machine designs. We perform this examination over the entire list of twelve machines. Reading across the columns of Table III for each row labeled α_i gives a measure of the uncertainty $\Delta\alpha_i$ in the empirical exponents. Reading down the columns shows in the first column the standard Kaye exponent with the predicted confinement times, and in the following columns the exponents describing the confinement without a particular machine. The last four rows give the numbers of shots in the columns, and the projected confinement times of the reference design values of IGNITOR, ITER-FEAT and ITER. In these three rows the bold faced numbers are the extreme minimum and maximun values corresponding to the 12 machines, with the machine labeling that column dropped from the database.

Thus for the IGNITOR, ITER-FEAT and ITER we have the ordered sequences of confinement time projections:

$$\begin{aligned}
\tau_{\mathrm{E}}(\mathrm{IGNITOR}) &= \{0.333, 0.336, 0.375, 0.376, 0.382, 0.384, \\
&\quad 0.384, 0.394, 0.395, 0.396, 0.415, 0.472\}, \qquad (2) \\
\tau_{\mathrm{E}}(\mathrm{ITER-FEAT}) &= \{0.99, 1.17, 1.26, 1.27, 1.28, 1.29, \\
&\quad 1.30, 1.30, 1.30, 1.33, 1.34, 1.48\}, \qquad (3) \\
\tau_{\mathrm{E}}(\mathrm{ITER}) &= \{1.41, 1.64, 1.74, 1.79, 1.79, 1.81, \\
&\quad 1.81, 1.81, 1.83, 1.84, 1.87, 2.14\}. \qquad (4)
\end{aligned}$$

The mean values are 0.386 s, 1.27 s and 1.79 s. The standard deviations are 0.04 s, 0.11 s and 0.17 s.

For IGNITOR we observe that PBXM tends to increase the predicted confinement time, while CMOD tends to decrease the confinement time. The lower bound and upper bound

are 0.333 s and 0.472 s. The fractional range of the extreme values, which is defined as $2(\tau_{\max} - \tau_{\min})/(\tau_{\max} + \tau_{\min})$, is 35%.

For ITER-FEAT we observe that PBXM also tends to increase the predicted confinement time, while TFTR tends to decrease the confinement time. The lower bound and upper bound are 0.99 s and 1.48 s. The fractional range of the extreme values are 40%.

For ITER we observe the same influence from PBXM as for IGNITOR and ITER-FEAT, that this machine tends to increase the confinement time, while TFTR tend to decrease the confinement time. The lower bound and upper bound are 1.41 s and 2.14 s. The fractional range of the extreme values are 41%.

That the relatively small number (31) of PBXM shots increases the confinement time may be due to its larger aspect ratio (~ 6) and strongly shaped (bean-like) flux surfaces.

For comparison, for a 68.3% confidence interval, assuming a normal distribution is $2\sigma_\tau/\overline{\tau}_E = 21\%$, 17%, and 19%.

III. FUSP Subdatabase

Much of the L-mode database contains discharges far from the conditions of interest for a high-field compact fusion reactor. This is due to the use of high energy neutral beam injection (NBI) to produce these plasmas in the database. The plasmas distribution in $\langle T_{\rm i}\rangle / \langle T_{\rm e}\rangle$ and $\langle n\rangle / n_{\rm GW}$ are shown with the histograms in Figure 1 and Figure 2. Here the Greenwald limit is defined as $n_{\rm GW} = \dfrac{I_{\rm p}}{\pi a^2}$, where $n_{\rm GW}$, $I_{\rm p}$ and a are in $10^{20}{\rm m}^{-3}$, MA and m respectively. Thus, there is often a significant high energy ion population in the NBI produced plasma which drives the system away from the thermodynamic plasma thermal equilibrium. Kadomtsev [8] emphasizes that this strong auxiliary heating generally increases the noise in the plasma. A quantitative example of this effect is given in Mazzucato and Nazikian [9], where the density fluctuation is shown to increase monotonously with NBI power in TFTR. For a review of the turbulent transport and how the phenomenon leads to a power law confinement time in

an auxiliary heated tokamak, see [10].

In Figure 1 the shots are from eight machines, *i.e.*, CMOD, D3D, JET, JT-60U, PBXM, PDX, TFTR, TSUPRA. All shots, except for one from TFTR, satisfy $\langle T_{\rm i}\rangle / \langle T_{\rm e}\rangle > 0.5$. There are 40 shots from JT-60U, 14 shots from PDX and 1 shot from TFTR satisfying $\langle T_{\rm i}\rangle / \langle T_{\rm e}\rangle > 1.5$.

¿From the vertical lines in Figure 2, we can see that all the machine design densities for the future plasma burning experiments are much higher than most of the data in the L-mode database. Here we use the machine-specific density units, the Greenwald limit, for densities from different machines. The Greenwald densities compared with the design densities for the proposed reactors are listed in Table IV.

Here we make a high density thermal subdatabase selected from L-mode data to have sift $< \left|\frac{\langle T_{\rm i}\rangle}{\langle T_{\rm e}\rangle}\right| < \frac{1}{\rm sift}$, where sift $= 0.5$ and $\dfrac{n}{n_{\rm GW}} > 0.5$ labeled as FUSP for the fusion power database. The FUSP database has 425 discharges from five tokamaks given in Table V. This FUSP database includes 163 shots from JET, 90 shots from JT60U, 1 shot from PBXM, 34 shots from PDX, 137 shots from TFTR. All these 425 shots are with no Helium; whether we apply the no-Helium condition or not does not affect the FUSP subdatabase.

FTU is not listed in Table V because all the shots from FTU are in the ohmic heating phase instead of L-phase. CMOD has an averaged density of $\langle n\rangle = 1.2\times 10^{20}{\rm m}^{-3}$, a small minor radius of $a = 0.22$ m, but a small averaged plasma current of $I_{\rm p} = 0.68$ MA, and the averaged Greenwald limit is $n_{\rm GW} = 4.5\times 10^{20}{\rm m}^{-3}$, therefore the Greenwald normalized density is around $\langle n\rangle / n_{\rm GW} = 0.27$. ASDEX, D3D and TSUPRA have some shots satisfying $\langle n\rangle / n_{\rm GW} = 0.5$, which have no $T_{\rm e}$ or $T_{\rm i}$ available.

We perform a linear regression fit for the parameters in Eq. (1) for the FUSP database using $\log\tau_{\rm E}$ and $\log\mu_i$. The result is

$$\tau_{\rm E}({\rm FUSP}) = 0.0535 M^{-0.09} R^{1.09} a^{0.20} \kappa^{0.94} B^{0.20} I^{1.01} \langle n\rangle^{0.22} P^{-0.70}. \tag{5}$$

Table VI shows the mean values and the standard deviations of the exponents α_i of the linear regression fit from the FUSP subdatabase, the projections to the proposed reactors and the comparison with Kaye *et al.* [1]. The most prominent difference in the FUSP database from the 97L formula is the emergence of a large α_B (0.20 ± 0.03) compared with (0.03 ± 0.02) for the database with 1312 shots. The decrease in α_R favors compact machines. Another change is in α_M which are thought to be less significant.

The mean values and the standard deviations of α_i are given in Table VI. The predictions for ITER-FEAT and IGNITOR, from Eq. (5) from the FUSP database are

$$\tau_{\mathrm{IGNITOR}}(\mathrm{FUSP}) = 0.508 \text{ s}, \tag{6}$$

$$\tau_{\mathrm{FEAT}}(\mathrm{FUSP}) = 0.94 \text{ s}. \tag{7}$$

The corresponding Lawson products for the machines are

$$\langle n \rangle \, \tau_{\mathrm{IGNITOR}}(\mathrm{FUSP}) = 2.5 \times 10^{20} \mathrm{m}^{-3}\mathrm{s}, \tag{8}$$

$$\langle n \rangle \, \tau_{\mathrm{FEAT}}(\mathrm{FUSP}) = 9.1 \times 10^{19} \mathrm{m}^{-3}\mathrm{s}. \tag{9}$$

IV. Discussion and Conclusion

¿From Table III we can see that the influence of the machines listed in Table V. Only JET has an influence of raising the confinement time and constitutes a considerable large fraction of the shots (163/425=38%). TFTR also has a considerable number of shots (137/425=32%), but lowers the projected confinement times. JT-60 and PDX data are relatively neutral, and could be dropped with a minor effect. Therefore, we can say that the changes of the predicted confinement times are due to the use of the FUSP subdatabase. The effect of using the FUSP database is to heavily weight the influence of JET and TFTR in making the prediction for the baseline confinement. This result, particularly the increase in α_B, which is essentially zero in the standard ITERL97-P formula, clearly shows the need for assembling a new, larger database of high-field, high-density, thermal plasma discharges.

The analysis shows that the confinement time predicted for IGNITOR by FUSP is increased by about 32% from the prediction by ITERL97P, while confinement time predicted for ITER-FEAT is decreased by 27%. The fact that there are relatively large errors in the power indices is attributable to the relatively small number of total shots for regression.

If we only apply the Greenwald criterion to the L-mode data with no Helium, the number of shots increases to 626. This dataset includes 41 shots from ASDEX, 15 shots from D3D, 228 shots from JET, 2 shots from JFT2M, 102 shots from JT60U, 1 shot from PBXM, 34 shots from PDX, 1 shot from T10, 138 shots from TFTR, 64 shots from TXTR. They are listed in Table VII. We have the projected confinement times 0.596 s, 0.883 s, 1.07 s, for IGNITOR, ITER-FEAT and ITER. For big-size machines, we see the decreases of the confinement times due principally to the change in α_R and α_B.

Figure 3(a) gives $\tau_{\rm measured}$ vs. $\tau_{\rm fit}$ for the FUSP subdatabase, which shows the degree of correlation of the data with the $\tau_{\rm E}$(FUSP) formula. That the probability distribution of the normalized confinement times is not so far from gaussian is shown in Figure 3(b). In Figure 3(b), we show the probability distribution function (pdf) of the measured confinement times $\tau_{\rm measured}$ normalized to the FUSP formula confinement time $\tau_{\rm FUSP}$. The probability distribution of this ratio is the so called H factor. For the data used to construct $\tau_{\rm E}$(FUSP) the mean value of $H_{\rm FUSP}$ is 1.00 by definition and the standard deviation is 0.11. The normalized ($H_{\rm FUSP}$) confinement time is weakly skewed distribution with skewness = 0.23 towards high confinement times ($H_{\rm FUSP} > 1$) and the kurtosis = 2.4 compared to 3.0 for a gaussian distribution. If the non-normal features are neglected, then the 95% confidence interval for the FUSP data is $\tau_{\rm E}(\text{FUSP}) \times (1.00 - 0.22, 1.00 + 0.22)$.

A preliminary comparison of the empirical formula $\tau_{\rm FUSP}$ for the H-mode data satisfying the $T_{\rm i}/T_{\rm e}$ and $\langle n \rangle / n_{\rm GW}$ conditions also shows a similar near-to-normal distribution with $\langle H \rangle = 1.86$ and $\sigma = 0.33$.

We recognize that these confinement times derived from the L-mode international database

are pessimistic. Advanced operational senarios are expected to provide enhancement factors of 2 or greater, from ELMy H-mode operation in a divertor system or from an internal transport barrier due to optimized or reversed magnetic shear profiles. Descriptions of these plasmas, however, require more parameters. Thus, the results given here are baseline tokamak confinement times. It is suggested that these times be view as lower bounds for the predicted confinement in the ITER-FEAT and IGNITOR.

Acknowledgments

We acknowledge the help of S. Kaye in acquiring and understanding the international ITER database.

This work was supported by the U.S. Dept. of Energy Contract No. DE-FG03-96ER-54346.

References

[1] Kaye, S.M., ITER Confinement Database Working Group, *et al.*, Nucl. Fusion **37**, (1997) 1303.

[2] Yushmanov, P.N., *et al.*, Nucl. Fusion **30**, (1990) 1999.

[3] Christiansen, J.P., *et al.* Nucl. Fusion **32**, (1992) 291.

[4] Coppi, B., A. Airoldi, F. Bombarda, G. Cenacchi, P. Detragiache, C. Ferro, R. Maggiora, L.E. Sugiyama, and G. Vecchi, Critical physics issues for ignition experiments: Ignitor, MIT (RLE) Report PTP 99/06.

[5] Lackner, K., and D. Campbell, ITER fusion energy advanced tokamak, document submitted to the CEA panel on thermonuclear fusion meeting, Paris, Nov. 25-26, 1999.

[6] ITER Physics Expert Group on Confinement and Transport and Database, *et al.*, Nucl. Fusion **39**, (1999) 2175.

[7] St. Petersburg Report of ITER Technical Advisory Committee Meeting, June 15, 2000.

[8] Kadomtsev, B.B., *Tokamak Plasma*, (IOP Publishing Ltd. 1992), pp. 124-147.

[9] Mazzucato, E., and R. Nazikian, Phys. Rev. Lett. **71**, (1993) 1840.

[10] Horton, W., Rev. Mod. Phys. **71**, (1999) 735.

FIGURE CAPTIONS

FIG. 1. Histogram of the ratios of the averaged ion temperature to the averaged electron temperature. The total number of shots shown is 707. The mean value of the ratio is 1.1 and the standard deviation is 0.3.

FIG. 2. Histogram of normalized electron density where the mean value is 0.49 and the standard deviation is 0.18.

FIG. 3. Correlation and pdf of the confinement time data normalized to the FUSP formula.

Table I: Map between physical variables and the symbols in the ITERL database.

Physical variables	Symbols in database	Units in power law
M_{eff}	MEFF	amu
R	RGEO	m
a	AMIN	m
κ	KAPPA	
B_{T}	BT	T
I_{P}	IP	MA
$\langle n \rangle$	NEL	$10^{19}\mathrm{m}^{-3}$
P_{L}	PLTH	MW
$\tau_{\mathrm{E,th}}$	TAUTH	s

Table II: Parameters for the proposed reactors.

	IGNITOR	ITER-FEAT	ITER
M_{eff} (amu)	2.5	2.5	2.5
R (m)	1.32	6.2	8.14
a (m)	0.47	2.0	2.8
κ	1.83	1.85	1.6
B_{T} (T)	13.	5.3	5.68
I_{p} (MA)	11.	15.1	21.0
$\langle n \rangle$ ($10^{19}\mathrm{m}^{-3}$)	62.	9.7	11.
P (MW)	24.7	120	216.
τ_{E} (s)	0.6	2.0	5.9

Table III: Looking for influential datasets.

	97P	ASDEX	CMOD	D3D	JET	JFT-2M
const	-3.78	-3.77	-3.76	-3.74	-3.80	-3.76
α_M	0.20	0.19	0.20	0.19	0.22	0.18
α_R	1.89	1.89	1.78	1.86	1.84	1.88
α_a	-0.06	-0.07	-0.06	-0.05	-0.10	-0.08
α_κ	0.64	0.62	0.64	0.71	0.58	0.64
α_B	0.03	0.02	0.08	0.01	0.01	0.03
α_I	0.96	0.97	0.98	0.97	0.91	0.97
$\alpha_{\langle n \rangle}$	0.40	0.41	0.42	0.40	0.38	0.38
α_P	-0.73	-0.74	-0.74	-0.73	-0.67	-0.72
# shots dropped	0	72	55	129	325	127
τ_{IGNITOR} (s)	0.384	0.384	**0.472**	0.395	0.336	0.376
τ_{FEAT} (s)	1.29	1.28	1.26	1.33	1.17	1.30
τ_{ITER} (s)	1.82	1.79	1.74	1.84	1.64	1.81

JT60	PBXM	PDX	T-10	TFTR	TSUPRA	TXTR
-3.77	-3.32	-3.86	-3.77	-4.06	-3.80	-3.77
0.21	0.09	0.21	0.20	0.26	0.21	0.20
1.91	1.54	1.94	1.90	2.04	1.90	1.88
-0.14	0.32	-0.09	-0.09	-0.06	-0.06	-0.05
0.59	0.54	0.68	0.63	0.68	0.64	0.64
0.00	0.09	0.05	0.02	0.07	0.03	0.04
1.02	0.91	0.97	0.98	0.89	0.96	0.95
0.39	0.41	0.40	0.39	0.47	0.40	0.40
-0.74	-0.77	-0.74	-0.73	-0.73	-0.73	-0.74
174	31	40	20	189	68	82
0.396	**0.333**	0.394	0.382	0.415	0.384	0.375
1.30	**0.99**	1.34	1.29	**1.48**	1.30	1.27
1.81	**1.41**	1.87	1.81	**2.14**	1.83	1.79

Table IV: Greenwald densities for the proposed reactors.

	$\langle n \rangle$ $(10^{19}\mathrm{m}^{-3})$	n_{GW} $(10^{19}\mathrm{m}^{-3})$	$\langle n \rangle / n_{\mathrm{GW}}$
FEAT	9.7	12.0	0.81
IGNITOR	62	159.	0.39
ITER	11	8.5	1.29

Table V: Discharges from FUSP subdatabase.

JET	JT60	PBXM	PDX	TFTR	total
163	90	1	34	137	425

Table VI: Linear regression fit from FUSP subdatabase and comparison with Kaye *et al.*[1]

	Kaye's 97P	FUSP
const	ln(0.023) ± 0.05	-2.93 ± 0.07
α_M	0.20 ± 0.02	-0.08 ± 0.03
α_R	1.89 ± 0.04	1.09 ± 0.07
α_a	-0.06 ± 0.04	0.20 ± 0.09
α_κ	0.64 ± 0.03	0.94 ± 0.08
α_B	0.03 ± 0.02	0.20 ± 0.03
α_I	0.96 ± 0.02	1.01 ± 0.04
$\alpha_{\langle n \rangle}$	0.40 ± 0.02	0.22 ± 0.04
α_P	-0.73 ± 0.009	-0.70 ± 0.02
# shots	1312	425
τ_{IGNITOR} (s)	0.384	0.508
τ_{FEAT} (s)	1.29	0.94
τ_{ITER} (s)	1.82	1.15

Table VII: Discharges from Greenwald database.

ASDEX	D3D	JET	JFT2M	JT60	PBXM	PDX	T10	TFTR	TXTR	total
41	15	228	2	102	1	34	1	138	64	626

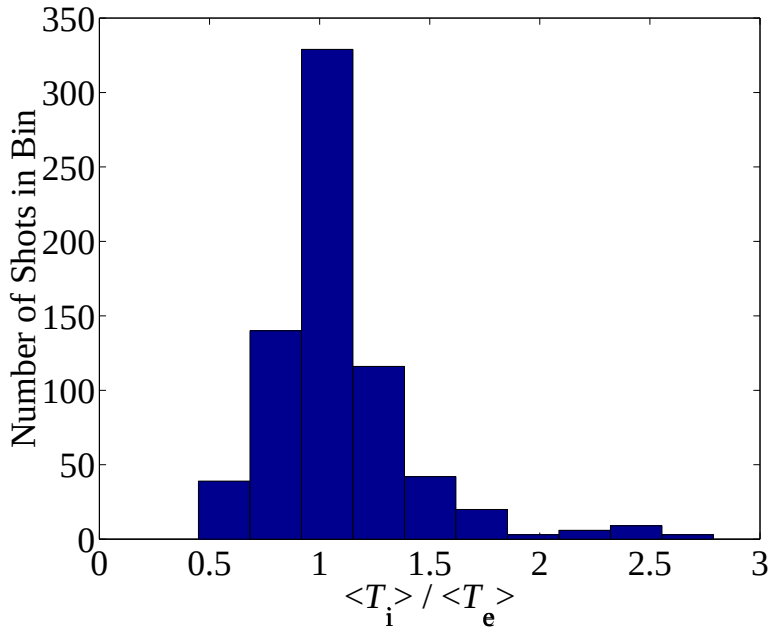
350
300
250
200
150
100
50
0
Number of Shots in Bin
0
0.5
1
1.5
2
2.5
3
<T_i> / <T_e>

Figure 1:

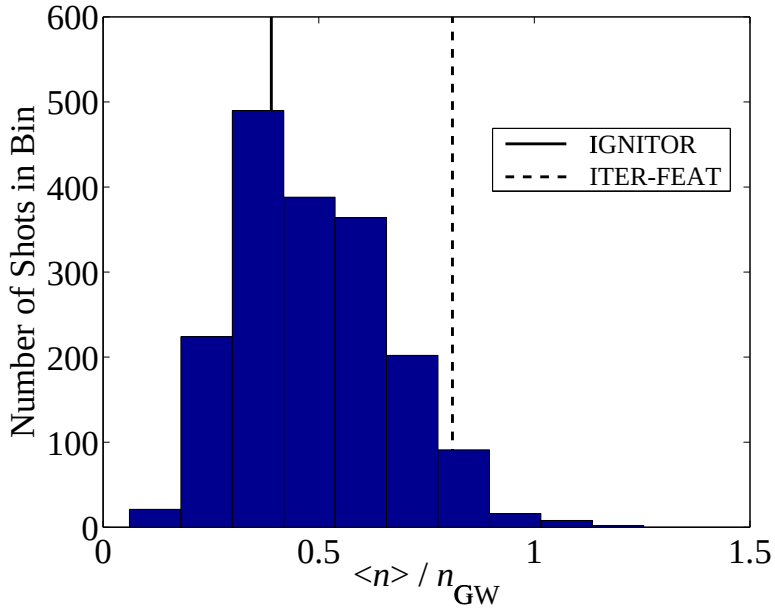
600
500
400
300
200
100
0
Number of Shots in Bin
0
0.5
1
1.5
<n> / n_GW
IGNITOR
ITER-FEAT

Figure 2:

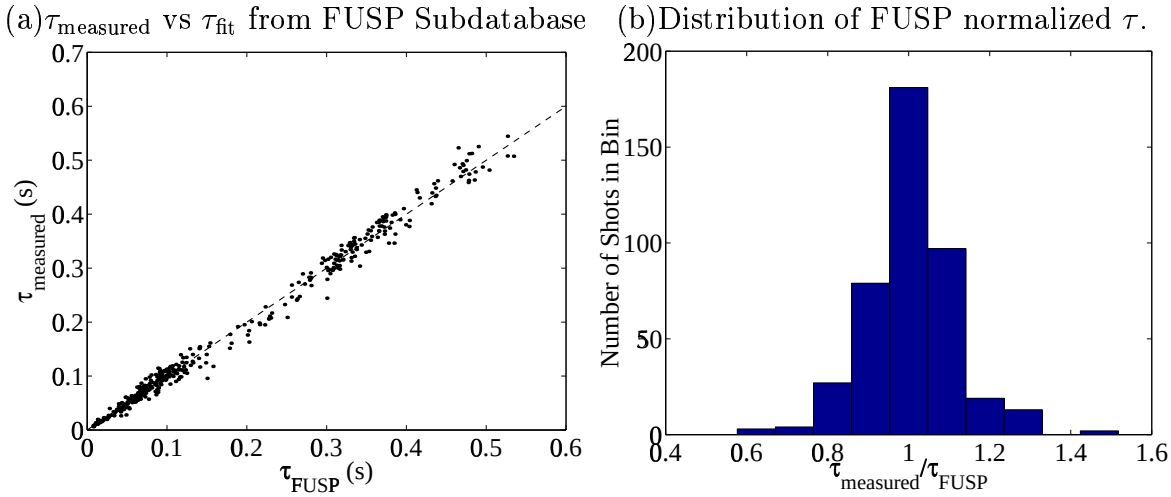
(a)τ_{measured} vs τ_{fit} from FUSP Subdatabase
(b)Distribution of FUSP normalized τ.
τ_{measured} (s)
τ_{FUSP} (s)
Number of Shots in Bin
$\tau_{\text{measured}}/\tau_{\text{FUSP}}$

Figure 3: